ELSEVIER

Journal of Nuclear Materials 289 (2001) 270–280

journal of nuclear materials

www.elsevier.nl/locate/jnucmat

# Oxygen potential and defect structure of the solid solution, Mg–Gd–$UO_2$

Takeo Fujino [a,*], Nobuaki Sato [a], Kohta Yamada [a], Manabu Okazaki [a], Kousaku Fukuda [b,1], Hiroyuki Serizawa [b], Tetsuo Shiratori [b]

[a] *Institute for Advanced Materials Processing, Tohoku University, 2-1-1 Katahira, Aoba-ku, Sendai 980-8577, Japan*

[b] *Japan Atomic Energy Research Institute, Tokai Research Establishment, Tokai-mura, Naka-gun, Ibaraki-ken 319-1195, Japan*

Received 22 May 2000; accepted 27 December 2000

**Abstract**

For solid solutions $Mg_yGd_zU_{1-y-z}O_{2+x}$ with $y = 0.03, 0.06$ and $0.10$ and $z = 0.142$, oxygen potential, $\Delta\bar{G}_{O_2}$, was measured as a function of O/M ratio (M = Mg+Gd+U) at temperatures between 1000°C and 1250°C. The O/M ratio which gives the steepest change of $\Delta\bar{G}_{O_2}$ (referred to as GOM) was lowered with increasing magnesium concentration. The GOMs were 1.968, 1.940 and 1.914 for 3, 6 and 10 mol% Mg, respectively. There seemed to be no temperature dependence of GOM. As the oxygen partial pressure, $p_{O_2}$, decreases, a part of the magnesium atoms rearrange from the substitutional 4*a* sites of $Fm\bar{3}m$ to the interstitial 4*b* sites as shown by density measurements, during which the magnesium solubility decreases from $y = 1/3$ to the minimum (<0.06) at around $p_{O_2} = 10^{-3}$ Pa. However, at $p_{O_2} = 10^{-8}$ Pa, the solubility again increases to >0.1. The ratio of interstitial magnesium to total magnesium was near 0.5 at 3–5 mol% Mg at GOM. The change rates of lattice parameter were found to be $\partial a/\partial x = -0.101$ Å, $\partial a/\partial y = +0.290$ Å for interstitial magnesium and $\partial a/\partial z = -0.187$ Å. © 2001 Elsevier Science B.V. All rights reserved.

*PACS:* 28.41.Bm

## 1. Introduction

A number of important improvements of the fuel performance in light water reactors have been made utilizing solid solution fuels. The gadolinium-doped $UO_2$ solid solution (hereafter referred to as gadolinium solid solution) is known as a burnable poison fuel, where the faster decrease of neutron absorber $^{155}Gd$ and $^{157}Gd$ on irradiation controls the change of the excess reactivity of the fuel during use. There are some differences in the thermodynamic properties of the gadolinium solid solution and undoped uranium dioxide. The gadolinium solid solution has an extended range of oxygen non-stoichiometry in both the O/M <2 (M = Gd + U) and $\geqslant 2$ regions [1,2]. This wide non-stoichiometric range of existence is in contrast to uranium dioxide of which the non-stoichiometry is limited to O/U $\geqslant$ 2 at temperatures below 1400°C [3,4]. The oxygen potential, $\Delta\bar{G}_{O_2}$, of the solid solution increases with increasing concentration of gadolinium. The rate of the $\Delta\bar{G}_{O_2}$ increment is about 3 kJ $mol^{-1}$ per 1 mol% Gd, which is almost unchanged by the O/M ratio in the hyperstoichiometric range [5]. According to the post-irradiation annealing experiments [6], the diffusion coefficient of $^{85}Kr$ in the gadolinium solid solution is low, close to that in $UO_2$ though it increases with increasing O/M ratio in the hyperstoichiometric range [7].

The thermodynamic properties of the solid solution doped with magnesium are significantly different from those of the gadolinium solid solution. The solubility of MgO in $UO_2$ is much lower than that of $Gd_2O_3$ under low oxygen partial pressures even at high temperatures

* Corresponding author. Tel.: +81-22 217 5163; fax: +81-22 217 5164.

*E-mail address:* fujino@ibis.iamp.tohoku.ac.jp (T. Fujino).

[1] Tel.: +81-29 282 5404; fax: +81-29 282 6441.


PII: S0022-3115(01)00427-5

above 2000°C [8,9]. On the other hand, on sintering $UO_2$ in the presence of MgO, larger grain sized pellets, which effect to lessen the FP gas release during irradiation [10], are formed. These data show the possibility of improvement of fuel performance of the gadolinium burnable poison fuel by the addition of magnesium.

The phase behavior of the MgO–$UO_2$–$O_2$ system is known to be somewhat complicated. Magnesium dissolves into $UO_2$ crystal up to 33.3 mol% when heated in relatively high oxygen partial pressures, e.g. of the order of 1 Pa [11,12]. However, the solubility decreases to around 4 mol% Mg at the oxygen pressures of $10^{-3}$–$10^{-4}$ Pa. If the oxygen pressure still decreases to $10^{-6}$ Pa, the solubility turns into increase. The solubility at the oxygen partial pressures of $10^{-8}$–$10^{-14}$ Pa was observed to exceed 10 mol% at 1200°C [13]. The above behavior is considered to be related to the change of the crystallographic position of magnesium in the solid solution. Foreign metal atoms usually substitute for uranium atoms in the 4*a* sites of the space group $Fm\bar{3}m$ of $UO_2$, and this is also the case for magnesium solid solution formed under higher oxygen partial pressures [12]. However at low oxygen partial pressures, a part of magnesium atoms occupy the interstitial sites [13,14], i.e., the 4*b* sites of the $Fm\bar{3}m$ space group, which are otherwise left vacant unless the solid solution is hyperstoichiometric. The minimum solubility of magnesium is thought to correspond to the transient state that the magnesium atoms rearrange their sites. That is to say, if the added amount of magnesium is smaller than the minimum solubility, magnesium never precipitates as MgO at any oxygen partial pressures. However, there is an important point to be clarified for Mg–Gd solid solution. It is the magnesium solubility in the presence of gadolinium in $UO_2$. Also, the oxygen potential of such a quaternary solid solution has not been reported.

In this work, each of 3, 6 and 10 mol% Mg was heated to dissolve into 14.2 mol% gadolinium solid solution. The composition of the quaternary solid solutions prepared under various heating conditions was precisely determined by chemical titration. The lattice parameter of the solid solution was obtained by X-ray diffractometry. Its change with the concentrations of (substitutional and interstitial) magnesium, gadolinium and non-stoichiometric oxygen was discussed. The density of the solid solution was measured pycnometrically. The variation of oxygen potential of the solid solution was studied as a function of O/M ratio, magnesium concentration and temperature. This quantity was discussed in terms of configurational entropy change due to the concentrations of magnesium (substitutional and interstitial) and oxygen non-stoichiometry.

## 2. Experimental

### 2.1. Materials used

Uranium metal turnings were dissolved in 6 M nitric acid. Purification of uranium was made by means of the TBP extraction method. After uranium was extracted by TBP, it was scrubbed with water and then with dilute ammonium carbonate solution. Ammonium diuranate precipitate, which was formed by adding ammonium hydroxide to the solution, was filtered off, dried and subsequently converted to $UO_3$ by heating in air at 500°C [15]. Stoichiometric $UO_2$ was obtained by heating $UO_3$ in a stream of hydrogen at 1000°C for 6 h. The main metallic impurities in the $UO_2$ analyzed by ICP method are listed in Table 1.

Guaranteed reagent heavy MgO (CaO <0.05%, heavy metals <0.005%) was purchased from Wako Pure Chemicals Industries. Gadolinium sesquioxide of 99.9% purity was obtained from Nippon Yttrium. Hydrogen gas of nine N purity was produced by a Whatman Model 75-34JA-100 hydrogen generator. Carbon dioxide and $N_2$ (99.99%) gases were obtained from Nippon Sanso and used as received.

### 2.2. Preparation of solid solution

The calculated amounts of MgO, $Gd_2O_3$ and $UO_2$ were intimately mixed in an agate mortar for about 40 min. The mixture was heated in air in a muffle furnace at 800°C for 3 days to change to uranates. The cycle of mixing and heating was repeated three times to obtain the well mixed oxides.

About 1 g of the air heated sample was pressed into a pellet of 10 mm$\varnothing$. Several pellets were heated together on an alumina boat in a horizontal SiC tube furnace at 1250°C for 2 days in a stream of $CO_2/H_2$ mixed gas with the mixing ratio of 450:1 (ml $min^{-1}$) using two mass-flow controllers (Kofloc, Type-3510 1/4SW-500SCCM and 1/4-10SCCM). The oxygen partial pressure was calculated to be 1.0 Pa by this gas ratio at 1250°C [16]. After the reaction, the pellets were crushed and mixed. The powder was pelletized and heated under the same conditions again. This cycle was repeated three times.

Table 1
Metallic impurities in $UO_2$

| Element | Amount (ppm) |
|---|---|
| Pd | 54 |
| Y | 2 |
| La | 4 |
| Tm | 94 |
| Th | 4 |

### 2.3. X-ray diffraction analysis

X-ray powder diffractometry was carried out with a Rigaku Type RAD-IC diffractometer using CuK$\alpha$ radiation (40 kV, 20 mA) monochromatized with curved pyrolytic graphite. The slit system used was 1°–0.5 mm–1°–0.15 mm. Measurements were made in a $2\theta$ range between 10° and 140° with a scanning rate of $1°(2\theta)$ per minute. The lattice parameter of the cubic solid solution was calculated by the least-squares method using the LCR2 program [17]. The precipitation of MgO phase in the solid solution was checked by step scanning (18 s counting time and $0.01°(2\theta)$ step width) in the range of $40.88° \leqslant 2\theta \leqslant 44.88°$ to detect the strongest diffraction peak of MgO at $42.8°(2\theta)$.

### 2.4. Chemical analysis

10–20 mg of solid solution powder was weighed with an accuracy of $\pm 10$ μg. The sample was dissolved in 5 ml of 0.05 M Ce(IV) solution in 1.5 M sulfuric acid by warming the solution to 80–90°C. The O/M ratio of the solid solution was determined by titrating the amount of excess Ce(IV) with Fe(II) ammonium sulfate solution using ferrion indicator [18,19]. The concentrations of Ce(IV) and Fe(II) solutions used were standardized by titration using stoichiometric $UO_2$. The estimated standard deviation in the measured O/M ratios was within $\pm 0.005$.

### 2.5. Oxygen potential measurements

#### 2.5.1. Method 1

2–3 g solid solution powder was pressed into pellets. The pellets with three different magnesium concentrations were placed on an alumina boat. They were subsequently heated in a horizontal SiC resistance tube furnace in a stream of $CO_2/H_2$ mixed gas. The mixing ratio of the gases was controlled with two mass-flow controllers in order to have the intended oxygen partial pressure calculated by the use of the literature $\Delta_f\bar{G}^\circ$ values for $H_2O$(g), $CO_2$(g) and CO(g) [16]. The samples were heated at a fixed temperature for 3–4 days to attain equilibrium. After the reaction, the whole system was evacuated by a rotary pump, and the current to the furnace was turned off. Calculation shows that the change of the O/M ratio during cooling was negligibly small. The O/M ratio of the cooled sample was determined by chemical analysis.

#### 2.5.2. Method 2

The solid solution sample (400–800 mg), whose O/M ratio had been determined by chemical analysis, was precisely weighed. The sample in a quartz basket was suspended from a Cahn-RG electrobalance by platinum wire. The whole system was evacuated with a rotary pump. After evacuating for 1 h, the stopcock connected to the rotary pump was closed, and the vacuum leak was checked by mercury manometer for several hours. Then, $N_2$ gas was slowly introduced into the system up to the ambient pressure. The $CO_2/H_2$ mixed gas was led to flow over the sample. The mixing ratio of the $CO_2/H_2$ gases was controlled with the mass-flow controllers to have an intended oxygen partial pressure at the heating temperature.

The sample was heated in a flow of the mixed gas. After no more weight change of the sample was observed for several hours, this weight was recorded, and the mixing ratio of the gases was changed for the next measurement. Above 1100°C, the measurements were carried out using a platinum basket instead of the quartz basket. Below the oxygen partial pressure of $10^{-11}$ Pa, nickel suspension wire and basket were used. After a series of measurements in the various oxygen partial pressures were finished, the sample was equilibrated with the oxygen partial pressure of $10^{-8}$ Pa at 1200°C. It was then evacuated by rotary pump followed by furnace cooling. Generally, the solid solutions are regarded to give the steepest change in the curve of oxygen potential versus O/M ratio around the above oxygen pressure at 1000–1200°C [20]. Therefore, after this O/M ratio was obtained in the thermogravimetric curve, the sample was cooled and chemical analysis for the composition was performed. The O/M ratios that had been measured by thermogravimetry were corrected using the O/M ratio for the steepest $\Delta\bar{G}_{O_2}$ change determined by titration.

### 2.6. Density measurement

The density of the solid solution was measured by the toluene displacement method. 2–3 g sample powder was measured in a glass bulb (7.423 g in weight with 2.861 ml inner volume) first in air and then in toluene at 25°C. To minimize the systematic error from open pores in the powder sample, the bulb containing the sample and toluene was put in a desiccator and carefully evacuated until bubble formation from the open pores ceased.

## 3. Results and discussion

### 3.1. Oxygen potential

The oxygen potential, $\Delta\bar{G}_{O_2}$, of Mg–Gd solid solution measured by method 1 at 1250°C is shown in Fig. 1 as a function of O/M ratio. Curve 1 (○), curve 2 (◇) and curve 3 (△) denote 3, 6 and 10 mol% Mg, respectively. The concentration of gadolinium is 14.2 mol%. In Fig. 1, the three curves show sigmoidal changes with O/M ratio. The steepest (vertical) change of $\Delta\bar{G}_{O_2}$ is seen to occur between $-400$ and $-300$ kJ mol$^{-1}$. These values are corresponding to $p_{O_2} = 1.9 \times 10^{-9}$ and $5.1 \times 10^{-6}$ Pa,

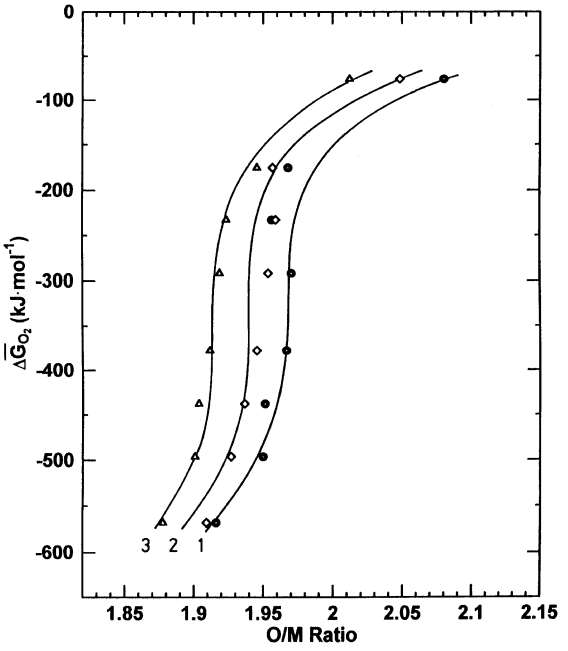


Fig. 1. Oxygen potential of Mg–Gd solid solution at 1250°C. Method 1, 14.2 mol% Gd, Curve 1: 3 mol% Mg, Curve 2: 6 mol% Mg, Curve 3: 10 mol% Mg.

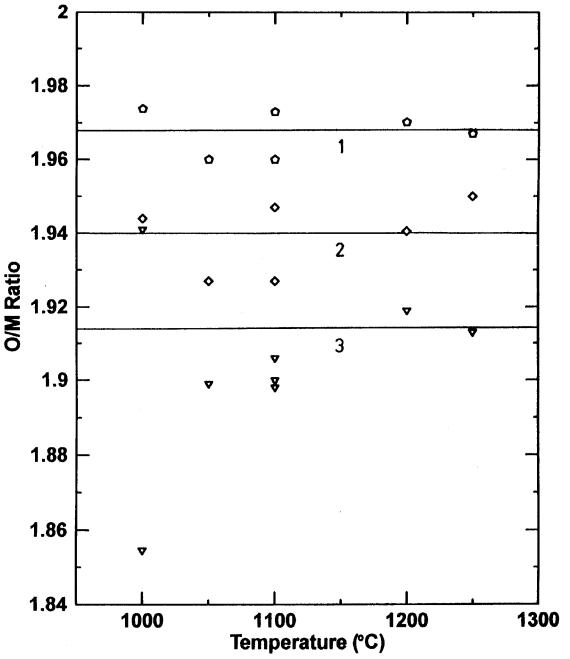


Fig. 2. O/M ratios for the steepest change of $\Delta\bar{G}_{O_2}$ plotted against temperature. Line 1, (⬠) 3 mol% Mg; Line 2, (◇) 6 mol% Mg; Line 3, (▽) 10 mol% Mg.

respectively. It is characteristic for all three curves that the O/M ratio which gives rise to the steepest change in $\Delta\bar{G}_{O_2}$, which will be referred to as GOM hereafter, shifts leftward from 2. This shift becomes larger as the magnesium concentration increases, indicating that magnesium is responsible for this phenomenon. The shift rate at GOM is about −0.007 or −0.008 (as O/M ratio) per 1 mol% Mg. It is noteworthy that the gadolinium solid solution does not yield any such shift. The steepest change of $\Delta\bar{G}_{O_2}$ takes place at O/M = 2 [1,2]. An interesting point is that the GOM shift of this kind occurs in magnesium solid solution and in europium solid solution though to a smaller degree. For the solid solution with 5 mol% Mg concentration, GOM is 1.989 at 1000°C [21]. For europium solid solution of 10 mol% Eu, GOM is 1.99 at 1250°C [22]. The GOMs observed in Fig. 1 are thus much smaller showing a peculiar feature of the Mg–Gd solid solution.

The GOM change with temperature was examined by method 1. The obtained data are listed in Table 2. In these experiments, the samples were heated for longer periods of 4–5 days to attain equilibrium. The obtained GOM data are plotted against temperature in Fig. 2. The marks ⬠, ◇ and ▽ show the values for 3, 6 and 10 mol% Mg, respectively. The values are scattered fairly largely, possibly because of low reaction rate for these high melting point oxides. Sintering of the pellets may also cause sluggishness of the reaction. The large difference in the two data at 1000°C for 10 mol% Mg solid solution suggests that the rate of rearrangement of magnesium from the substitutional to interstitial position is low at the lower temperature of 1000°C. The figure shows that there is no systematic temperature dependence of GOM in the present temperature ranges. The three horizontal lines of 1, 2 and 3 in Fig. 2, which are for 3, 6 and 10 mol% Mg, respectively, depict the averaged GOM's, i.e. 1.968, 1.940 and 1.914. The X-ray step scanning measurements revealed no formation of MgO precipitate in all specimens in Table 2 for which the X-ray diffraction analysis was carried out.

Fig. 3(a) is an example of the step scanned X-ray diffraction pattern in the $2\theta$ range from 40.88° to 44.88° for the Mg–Gd sample of 10 mol% Mg which was formed by heating at 1250°C under the oxygen partial pressure of $10^{-3}$ Pa for 4 days. An X-ray peak of MgO is seen at 42.83°. Fig. 3(b) is the step scanned result for the Mg–Gd sample of 10 mol% Mg heated at 1250°C under $p_{O_2} = 10^{-8}$ Pa. In this case, no X-ray peak of MgO can be detected. The solid solution is seen to be again in a single phase at this lower oxygen partial pressure.

The X-ray step scanning patterns for the specimens of different magnesium concentrations are shown in Fig. 4. The samples are those heated at $p_{O_2} = 10^{-3}$ Pa and 1250°C. Fig. 4(a) is the same pattern as Fig. 3(a) for 10 mol% Mg. Although MgO is precipitated at 10 mol% Mg, the peak of MgO can barely be detected at 6 mol%

Table 2
$\Delta\bar{G}_{O_2}$, O/M ratios and lattice parameters corresponding to the steepest change of $\Delta\bar{G}_{O_2}$

| Heating no. | Mg (mol%) | Temperature (°C) | $p_{O_2}$ (Pa) | $\Delta\bar{G}_{O_2}$(kJ mol$^{-1}$) | O/M ratio | a (Å) | $-x/2y$[a] | X-ray[b] |
|---|---|---|---|---|---|---|---|---|
| 1 | 3 | 1000 | $10^{-8}$ | −316.8 | 1.974 | $5.4418 \pm 0.0002$ | 0.433 | F2,s |
| 3 | 3 | 1050 | $10^{-8}$ | −329.3 | 1.960 | – | 0.667 | |
| 4 | 3 | 1100 | $10^{-8}$ | −341.7 | 1.960 | $5.4426 \pm 0.0001$ | 0.667 | S,s |
| 6 | 3 | 1100 | $10^{-10}$ | −394.3 | 1.973 | $5.4431 \pm 0.0001$ | 0.450 | S,s |
| 7 | 3 | 1200 | $2.1 \times 10^{-9}$ | −385.6 | 1.970 | $5.4427 \pm 0.0002$ | 0.500 | S,s |
| 8 | 3 | 1250 | $10^{-8}$ | −379.0 | 1.968 | – | 0.533 | |
| 1 | 6 | 1000 | $10^{-8}$ | −316.8 | 1.944 | $5.4408 \pm 0.0002$ | 0.467 | S,s |
| 3 | 6 | 1050 | $10^{-8}$ | −329.3 | 1.927 | – | 0.608 | |
| 4 | 6 | 1100 | $10^{-8}$ | −341.7 | 1.947 | $5.4413 \pm 0.0002$ | 0.442 | S,b |
| 6 | 6 | 1100 | $10^{-10}$ | −394.3 | 1.927 | $5.4417 \pm 0.0001$ | 0.608 | S,s |
| 7 | 6 | 1200 | $2.1 \times 10^{-9}$ | −385.6 | 1.941 | $5.4420 \pm 0.0001$ | 0.492 | S,s |
| 8 | 6 | 1250 | $10^{-8}$ | −379.0 | 1.950 | – | 0.417 | |
| 1 | 10 | 1000 | $10^{-8}$ | −316.8 | 1.941 | $5.4353 \pm 0.0004$ | 0.295 | S?,b |
| 2 | 10 | 1000 | $10^{-8}$ | −316.8 | 1.855 | – | 0.725 | |
| 3 | 10 | 1050 | $10^{-8}$ | −329.3 | 1.899 | – | 0.505 | |
| 4 | 10 | 1100 | $10^{-8}$ | −341.7 | 1.907 | $5.4377 \pm 0.0001$ | 0.465 | S,b |
| 5 | 10 | 1100 | $10^{-8}$ | −341.7 | 1.900 | – | 0.500 | |
| 6 | 10 | 1100 | $10^{-10}$ | −394.3 | 1.898 | $5.4395 \pm 0.0002$ | 0.510 | S,s |
| 7 | 10 | 1200 | $2.1 \times 10^{-9}$ | −385.6 | 1.919 | $5.4410 \pm 0.0002$ | 0.405 | S,s |
| 8 | 10 | 1250 | $10^{-8}$ | −379.0 | 1.913 | – | 0.435 | |

[a] Theoretical ratio of interstitial magnesium atoms to the total magnesium atoms (see Section 3.5).
[b] F2: Fluorite two phases; S: Fluorite single phase; S?: Possibly fluorite single phase; s: Sharp X-ray diffraction peaks; b: Broad X-ray diffraction peaks.

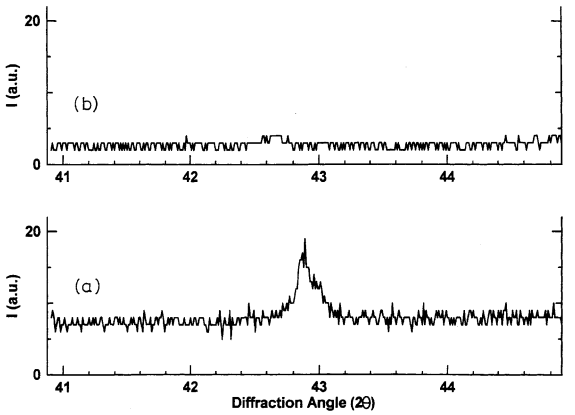


Fig. 3. Step scanned X-ray patterns for the samples of 10 mol% Mg. (a) $p_{O_2} = 10^{-3}$ Pa, 1250°C; (b) $p_{O_2} = 10^{-8}$ Pa, 1250°C.

Mg (Fig. 4(b)). Fig. 4(c) shows the pattern for 3 mol% Mg sample, where clearly no MgO peak exists. The solubility of magnesium in $UO_2$ is found to be between 3 and 6 mol% close to the latter even if the oxygen partial pressure is $10^{-3}$ Pa.

The $\Delta\bar{G}_{O_2}$ values obtained for 10 mol% Mg–14.2 mol% Gd solid solution are plotted against O/M ratio in Fig. 5 taking temperature as a parameter. Curves 1, 2 and 3 express the $\Delta\bar{G}_{O_2}$ change at 1000, 1100 and 1250°C, respectively. The curves are those corrected for the averaged GOM described above. The data points of △ and ◇ were obtained by method 1, and □ and ○ by method 2 (thermogravimetry). Curve 3 in Fig. 5 is the re-plot of curve 3 in Fig. 2.

It is seen from Fig. 5 that the oxygen potential at 1000°C is higher than those at 1100°C and 1250°C below

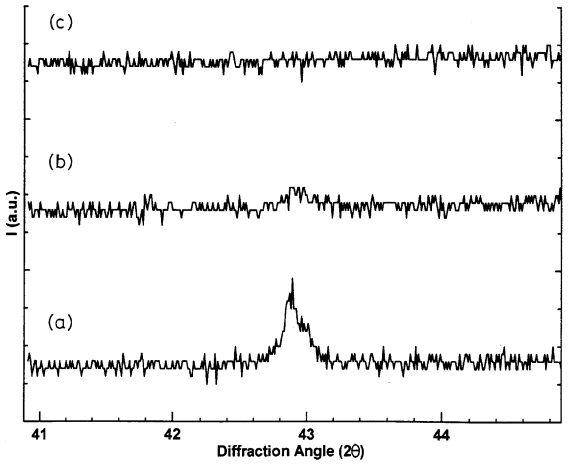


Fig. 4. Step scanned X-ray patterns for the samples heated at $p_{O_2} = 10^{-3}$ Pa at 1250°C. (a) 10 mol% Mg, (b) 6 mol% Mg, (c) 3 mol% Mg.

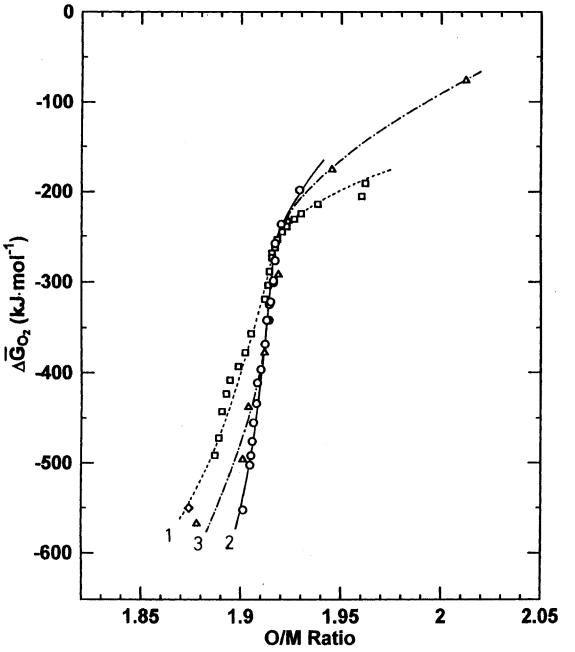


Fig. 5. Variation of oxygen potential with O/M ratio at 1000°C, 1100°C and 1250°C. Curve 1, (- - - -) 1000°C; Curve 2, (–) 1100°C; Curve 3, (–·–) 1250°C; (△) and (◇) Method 1; (□) and (○) Method 2.

GOM. This change by temperature is not in accord with that for gadolinium solid solution, where the $\Delta\bar{G}_{O_2}$ values at 1000°C are much lower than those at 1500°C [1,2]. It might be related to the reaction rate of the rearrangement of magnesium which is low and decreases significantly at a lower temperature of 1000°C. Since the thermogravimetric measurements were made in a direction from higher $\Delta\bar{G}_{O_2}$ to lower $\Delta\bar{G}_{O_2}$, there is a possibility that the concentration of substitutional magnesium is higher than that of equilibrium in the solid solution when heated at the lower temperature of 1000°C due to incomplete transformation. In the thermogravimetric measurements, the acquisition of each point at the intended oxygen partial pressure was made after no weight change of the sample was observed during several hours. It took about one day to measure one thermogravimetric point.

Fig. 5 shows that the $\Delta\bar{G}_{O_2}$ values at 1000°C above GOM are lower than those at 1100°C and 1250°C, which is consistent with the most other ternary solid solutions. The oxygen potentials at 1100°C are a little higher than those at 1250°C. This result is probably attributable to the experimental error in the thermogravimetric measurements. The oxygen potentials of the present solid solution can be compared with those of gadolinium solid solution at the O/M ratio larger than GOM by 0.01. The present solid solution with 10 mol%

Mg gives $\Delta\bar{G}_{O_2}$ near $-200$ kJ mol$^{-1}$ at 1000–1250°C. The oxygen potential of $Gd_{0.27}U_{0.73}O_{2+x}$ at O/M = 2.01 at 1500°C is around $-120$ kJ mol$^{-1}$[2].

### 3.2. Partial molar entropy and enthalpy of oxygen as a function of O/M ratio

Assuming that the partial molar entropy of oxygen ($\Delta\bar{S}_{O_2}$) and enthalpy ($\Delta\bar{H}_{O_2}$) do not change with temperature, their values for 10 mol% Mg–14.2 mol% Gd solid solution were calculated from the $\Delta\bar{G}_{O_2}$ in the O/M range above GOM at 1000°C and 1250°C in Fig. 5 using the relations

$$\Delta\bar{S}_{O_2} = \frac{-\partial\bar{G}_{O_2}}{\partial T} \quad \text{and} \quad \Delta\bar{H}_{O_2} = \frac{\partial(\Delta\bar{G}_{O_2}/T)}{\partial(1/T)}.$$

In Fig. 6, the change of the obtained $\Delta\bar{S}_{O_2}$ with O/M ratio for this solid solution is compared with the retrieved reference values for magnesium solid solution with 5 mol% Mg [21] (dashed line), gadolinium solid solution with 14 mol% Gd [2] (dash-dotted line) and europium solid solution with 5 mol% Eu [22] (dotted line). The solid curve for the present 10 mol% Mg–14.2 mol% Gd solid solution is consistent with the curves for the other solid solutions in Fig. 6 that $\Delta\bar{S}_{O_2}$ increases with decreasing O/M ratio above GOM, apart from the O/M ratio itself. Also, the $\Delta\bar{S}_{O_2}$ values of these curves are fairly close, showing that the temperature dependences of $\Delta\bar{G}_{O_2}$ for these solid solutions are alike. The reference three curves steeply decrease with decreasing O/M ratio below GOM. For the present Mg–Gd solid solution, although the curve is not extended to this region, the same is assumed to occur if the equilibrium is completely attained.

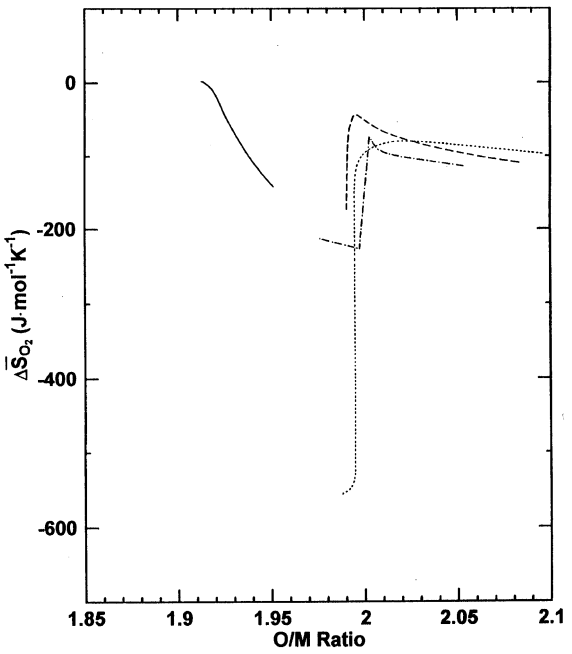


Fig. 6. $\Delta\bar{S}_{O_2}$ as a function of O/M ratio. (—) Present Mg–Gd solid solution with 10 mol% Mg, (– –) $Mg_{0.05}U_{0.95}O_{2+x}$ [23], (–·) $Gd_{0.14}U_{0.86}O_{2+x}$ [2], (···) $Eu_{0.05}U_{0.95}O_{2+x}$ [24].

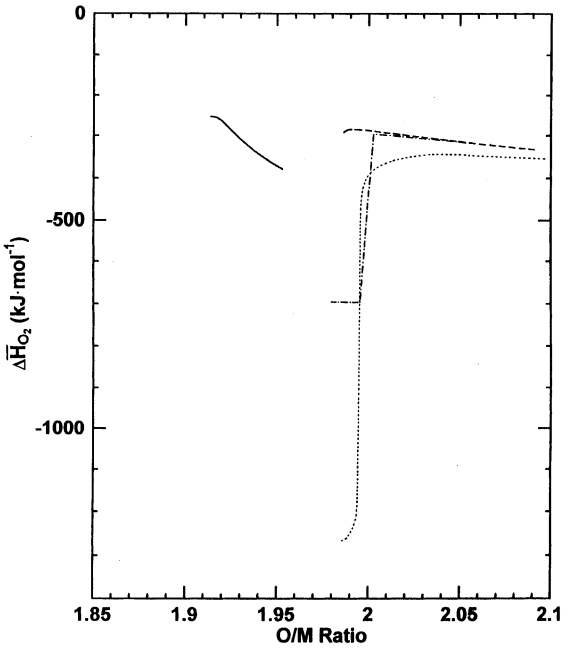


Fig. 7. $\Delta\bar{H}_{O_2}$ as a function of O/M ratio. (—) Present Mg–Gd solid solution with 10 mol% Mg, (– –) $Mg_{0.05}U_{0.95}O_{2+x}$ [23], (–·) $Gd_{0.14}U_{0.86}O_{2+x}$ [2], (···) $Eu_{0.05}U_{0.95}O_{2+x}$ [24].

Fig. 7 shows the partial molar enthalpy of oxygen for the same 10 mol% Mg–14.2 mol% Gd solid solution. In the figure, the enthalpies of magnesium solid solution with 5 mol% Mg [21], gadolinium solid solution with 14 mol% Gd [2] and europium solid solution with 5 mol% Eu [22] are also drawn for comparison as dashed, dash-dotted and dotted lines, respectively. It is seen from the figure that the $\Delta\bar{H}_{O_2}$ curves are similar in shape to the $\Delta\bar{S}_{O_2}$ curves. That is to say, the variation of $\Delta\bar{H}_{O_2}$ is specified by the rightmost term of the relation $\Delta\bar{H}_{O_2} = \Delta\bar{G}_{O_2} - T\partial\bar{G}_{O_2}/\partial T$. As in the case of $\Delta\bar{S}_{O_2}$, $\Delta\bar{H}_{O_2}$ increases with decreasing O/M ratio in the O/M range above GOM. Regarding $\Delta\bar{S}_{O_2}$ and $\Delta\bar{H}_{O_2}$ of Mg–Gd solid solution, both their feature and value are comparable with those of the other solid solutions cited in Figs. 6 and 7.

### 3.3. Density and defect type of the solid solution

In Fig. 8, the density of the Mg–Gd solid solution measured by the toluene displacement method is shown as a function of magnesium concentration (mol%). The circles and pentagons express the data for the three

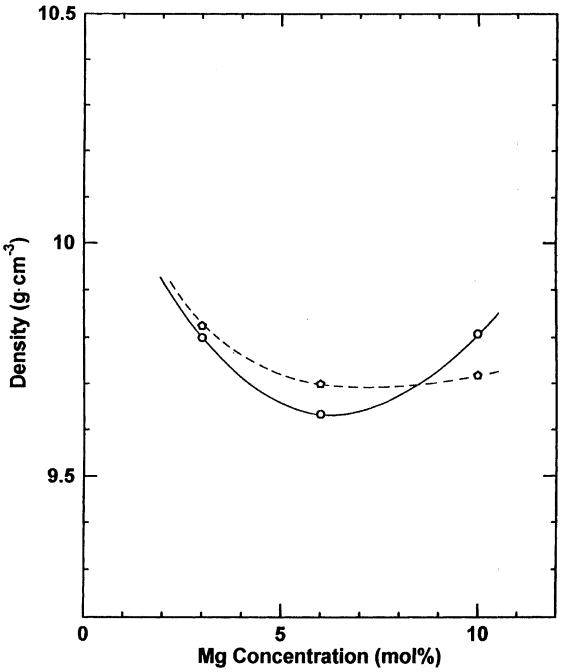


Fig. 8. Densities measured by toluene displacement method. (○) $p_{O_2} = 2.1 \times 10^{-9}$ Pa, 1250°C; (⬠) in $H_2$($p_{O_2} = 10^{-14}$–$10^{-16}$ Pa), 1000°C.

samples of heating number 7 in Table 2 and for those heated in an $H_2$ stream at 1000°C for 4 days, respectively. As is seen from Table 2, the former samples heated at $p_{O_2} = 2.1 \times 10^{-9}$ Pa and 1200°C were in a single phase. The latter samples were also single phase solid solutions with good crystallinity as analyzed by X-ray diffractometry. The lattice parameters and the O/M ratios were $a = 5.4458 \pm 0.0001$ Å and O/M = 1.946 for 3 mol% Mg, $a = 5.4449 \pm 0.0001$ Å and O/M = 1.913 for 6 mol% Mg, and $a = 5.4426 \pm 0.0001$ Å and O/M = 1.874 for 10 mol% Mg (Table 3). The oxygen potentials of the latter three samples are estimated to be in a range between −510 and −460 kJ $mol^{-1}$.

The density curves of Fig. 8 are seen to decrease with increasing magnesium concentration from 3 to 6 mol%, but both curves turn to increase above 6 mol%. For density calculation, the lattice parameter should be taken into account, but the density change with magnesium concentration in the figure does not seem to be caused by substituted magnesium which is much lighter than uranium. Table 4 compares the observed densities with three calculated densities for substitutional magnesium, interstitial magnesium and 50% substitutional–50% interstitial magnesium. For calculating the theoretical densities, all gadolinium atoms were placed in the substitutional sites. As the lattice parameters and

Table 3
O/M ratios and lattice parameters of the solid solutions formed by heating under low oxygen partial pressure of dry $H_2$ streams ($p_{O_2} = 10^{-14}$–$10^{-16}$ Pa) at 1000°C for 4 days

| Mg mol% | O/M ratio | Lattice parameter (Å) | $-x/2y$[a] | Remarks[b] |
|---|---|---|---|---|
| 3 | 1.946 | $5.4458 \pm 0.0001$ | 0.900 | S,s |
| 6 | 1.913 | $5.4449 \pm 0.0001$ | 0.725 | S,s |
| 10 | 1.874 | $5.4426 \pm 0.0001$ | 0.630 | S,s |

[a] Theoretical ratio of interstitial magnesium atoms to the total magnesium atoms (see Section 3.5).
[b] S: Fluorite single phase with no MgO precipitation; s: Sharp X-ray diffraction peaks.

Table 4
Observed densities in comparison with the calculated densities

| | Observed density (g $cm^{-3}$) | Calculated density (g $cm^{-3}$) | | |
|---|---|---|---|---|
| | | Sub.[a] | Int.[b] | 50%S–50%I[c] |
| Sample preparation 1[d] | | | | |
| 3 mol% Mg | 9.80 | 10.37 | 10.69 | 10.53 |
| 6 mol% Mg | 9.63 | 10.09 | 10.73 | 10.40 |
| 10 mol% Mg | 9.81 | 9.73 | 10.81 | 10.24 |
| Sample preparation 2[e] | | | | |
| 3 mol% Mg | 9.83 | 10.14 | 10.45 | 10.29 |
| 6 mol% Mg | 9.70 | 10.05 | 10.70 | 10.37 |
| 10 mol% Mg | 9.72 | 9.69 | 10.77 | 10.20 |

[a] All Mg atoms in substitutional sites.
[b] All Mg atoms in interstitial sites.
[c] 50% Mg in substitutional sites and 50% Mg in interstitial sites.
[d] $p_{O_2} = 2.1 \times 10^{-9}$ Pa at 1200°C for 4 days.
[e] $p_{O_2} = 10^{-14}$–$10^{-16}$ Pa at 1000°C for 4 days.

Table 5
Observed density calculated as a percent of theoretical density (TD)

| | Substitutional | Interstitial | 50% Sub.–50% Int. |
|---|---|---|---|
| Sample preparation 1[a] | | | |
| 3 mol% Mg | 94.5 | 91.7 | 93.1 |
| 6 mol% Mg | 95.5 | 89.8 | 92.6 |
| 10 mol% Mg | 100.8 | 90.8 | 95.8 |
| Sample preparation 2[b] | | | |
| 3 mol% Mg | 96.9 | 94.0 | 95.5 |
| 6 mol% Mg | 96.5 | 90.7 | 93.6 |
| 10 mol% Mg | 100.3 | 90.3 | 95.3 |

[a] $p_{O_2} = 2.1 \times 10^{-9}$ Pa at 1200°C for 4 days.
[b] $p_{O_2} = 10^{-14} - 10^{-16}$ Pa at 1000°C for 4 days.

O/M ratios, those in Table 2 (heating number 7) and Table 3 were used. Table 4 shows that the calculated density for substitutional magnesium decreases with increasing magnesium concentration while that for interstitial magnesium increases with increasing magnesium concentration as expected. Note that the observed (pycnometric) densities except for those of substitutional 10 mol% Mg samples are lower than the calculated (X-ray) densities. It is usually the case that the observed densities are several percent lower than the calculated densities due to closed pores in the specimens. That is to say, the substitutional solid solution is to be excluded.

The observed density was represented as the percent of theoretical density (% density). Table 5 tabulates the observed % densities for three magnesium positions. First, the possibility that all magnesium atoms are in substitutional sites is clearly denied, since the densities in the table for 10 mol% Mg exceed 100% for both conditions of sample preparation, 1 and 2. In the remaining two cases, the interstitial solid solution in Table 5 gives the % density which slightly decreases with increasing magnesium concentration. This change is more distinct for sample preparation 2, although the % density should be basically unvaried. Also, the % densities around 90% seem to be too low as the ones resulted from the closed pores since their concentration is generally several %. Therefore, the most possible solid solution is the one with 50% substitutional–50% interstitial magnesium. This result is in accord with the statistical thermodynamical calculation of $\Delta\bar{G}_{O_2}$, namely, $\Delta\bar{G}_{O_2}$ is predicted to be very high for interstitial magnesium solid solution and very low for 50% substitutional–50% interstitial magnesium solid solution [23]. The interstitial magnesium atoms occupy the 4*b* sites of the space group $Fm\bar{3}m$, and the remaining 50% magnesium atoms and all gadolinium atoms occupy the 4*a* substitutional sites statistically. The density measurements do not specify the interstitial/substitutional ratio to be one. This ratio was taken from [23] as the most stable ratio for the substitutional–interstitial solid solution in which all uranium atoms are in the tetravalent state. As will be discussed later in Section 3.5, this ratio can be changed depending on the heating condition.

### 3.4. Lattice parameter as a function of metal concentration and oxygen non-stoichiometry

In order to examine the lattice parameter change with composition, calculation was made using the experimental data of Tables 2 and 3. These solid solutions did not precipitate MgO. First, least-squares calculation was performed in order to have a linear relation between lattice parameter and O/M ratio for each of the three magnesium concentrations of 3, 6 and 10 mol% Mg. The obtained rates of the change of lattice parameter with O/M ratio were −0.1122, −0.0999 and −0.0906 Å for 3, 6 and 10 mol% Mg, respectively. Although the absolute value of the rate looks like to decrease with increasing magnesium concentration, it was difficult to find some meaning in this sequence. Then, the average of the three rates, i.e. −0.101 Å was taken in this work.

Using this rate, the next least-squares calculation was performed to have the lattice parameter at O/M = 2 for each of three magnesium concentrations. They were 5.4396, 5.4355 and 5.4290 Å for 3, 6 and 10 mol% Mg, respectively. The variation of the lattice parameter with magnesium concentration is depicted in Fig. 9. A good linearity was obtained in the figure suggesting that no peculiar change occurs in the defect type with magnesium concentration. Extrapolation of the straight line in Fig. 9 to 0 mol% Mg gives 5.4438 Å which should be the lattice parameter of stoichiometric gadolinium solid solution, $Gd_zU_{1-z}O_2$. By taking 5.4704 Å as the lattice parameter of stoichiometric uranium dioxide, the change rate of lattice parameter with gadolinium, $\partial a/\partial z$, is obtained as $(5.4438 - 5.4704)/0.142 = -0.187$ Å. The change rate of the lattice parameter with magnesium, $\partial a/\partial y$, can also be obtained from the slope of the line using the lattice parameters for 0 and 10 mol% Mg. The obtained rate −0.139 Å is considered to be the arithmetical average of the contributions of substitutional magnesium and interstitial magnesium. If the existence

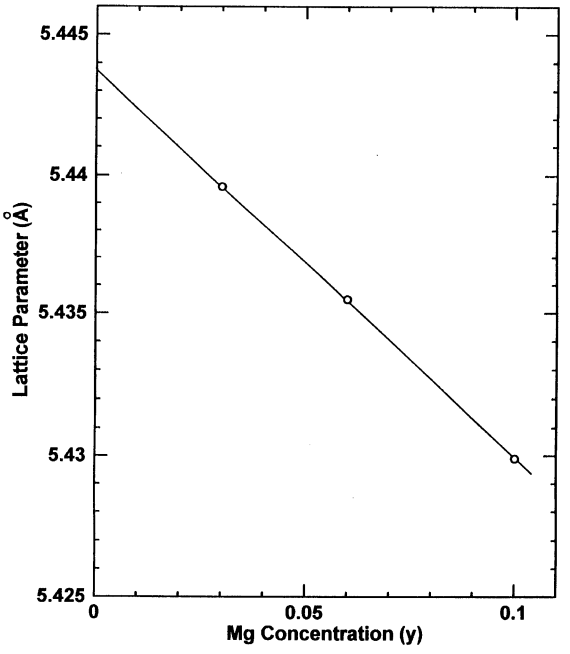


Fig. 9. Variation of lattice paremeter of Mg–Gd solid solutions with magnesium concentration at O/M = 2. Gd: 14.2 mol%.

ratio of these magnesium atoms is one, and the change rate of the lattice parameter by the substitutional magnesium is taken as −0.5677 Å [15], the $\partial a/\partial y$ factor of the interstitial magnesium is calculated to be +0.290 Å. The small change in the lattice parameter of magnesium solid solution with magnesium concentration at low oxygen partial pressures is understood as due to the effect of the formed interstitial magnesium having such a large positive rate.

The change rate of lattice parameter with O/M ratio, −0.101 Å, obtained in this work can be compared with those for the other solid solutions in hyperstoichiometric range. The $\partial a/\partial x$ rates are −0.14 Å for thorium solid solution [25], −0.131 Å for lanthanum solid solution [26], −0.127 Å for praseodymium solid solution [27], −0.112 Å for neodymium solid solution [28], −0.117 Å for magnesium solid solution [12], −0.102 Å for calcium solid solution [29] and −0.109 Å for strontium solid solution [30]. The change rate of lattice parameter with gadolinium concentration in this work, $\partial a/\partial z = -0.187$ Å, is comparable with the reference values of −0.164 [31], −0.173 [32] and −0.171 Å [33]. The rate theoretically estimated [22], −0.180 Å, is the closest to the present value.

Since the change rate of lattice parameter with interstitial magnesium, +0.290 Å, was calculated by assuming that the solid solution is of the type 50% substitutional −50% interstitial magnesium, this value changes with the substitutional to interstitial ratio of magnesium. Interstitial magnesium is characteristic in giving a large positive rate. The positive change rates on metal addition are known for thorium solid solution [25], lanthanum solid solution [26], bismuth solid solution [33], etc., but they are rather rare cases. Also, the above metals occupy the substitutional sites. For the solid solution containing magnesium, a part of magnesium atoms occupy the interstitial sites with a positive change rate, which is assumed to be realized with the coexistence of the substitutional magnesium atoms having a large negative change rate.

### 3.5. Relation of GOM, magnesium position and oxygen non-stoichiometry

If the ratio of interstitial $Mg^{2+}$ to the total $Mg^{2+}$ atoms is $m$ in the solid solution $Mg_yGd_zU_{1-y-z}O_{2+x}$, the formula is rewritten as $Mg^{2+}_{(1-m)y}Gd^{3+}_zU^{4+}_{1-2x-3y-2z}U^{5+}_{2x+2y+z}\{Mg^{2+}_{my}\}O^{2-}_{2+x}$, where the braces show the interstitial magnesium. Since the 4*a* sites of $Fm\bar{3}m$ are considered to be fully occupied by the metal atoms in this solid solution, the above formula should be divided by $1-my$ as

$$(1-my)\ Mg^{2+}_{\frac{(1-m)y}{1-my}}Gd^{3+}_{\frac{z}{1-my}}U^{4+}_{\frac{1-2x-3y-2z}{1-my}}U^{5+}_{\frac{2x+2y+z}{1-my}}\left\{Mg^{2+}_{\frac{my}{1-my}}\right\}O^{2-}_{\frac{2+x}{1-my}}. \quad (1)$$

Calculation of configurational $\bar{S}_{O_2}$ leads to give

$$m = \frac{-x}{2y} \quad (2)$$

as the most stable $m$ value thermodynamically predicted in the region of $x < 0$ [34]. If the relation of Eq. (2) holds in the crystal, the solid solution has no oxygen non-stoichiometry at any $x$ values in the $x < 0$ region [34], i.e., $(2+x)/(1-my)$ in Eq. (1) becomes 2. This is not true for the present Mg–Gd–$UO_2$ solid solution since the lattice parameter change as a function of O/M ratio, $2+x$, was observed and the change rate $\partial a/\partial x$ was in agreement with those of the other solid solutions as described in Section 3.4. Eq. (2) might be valid only around the O/M ratio which brings about the steepest change in $\Delta\bar{G}_{O_2}$ (Table 2). The GOM values were 1.968, 1.940 and 1.914 for 3, 6 and 10 mol% Mg, respectively. Using the above GOM values, 0.533, 0.500 and 0.430 were obtained as the $m$ values from Eq. (2). In this sequence, the value decreases slightly with increasing magnesium concentration, suggesting the difficulty for magnesium to occupy the interstitial sites up to high concentrations.

The rate of the lattice parameter change with O/M ratio, −0.101 Å, obtained for the present solid solution is comparable with those of the other solid solutions in the hyperstoichiometric range, although the data of Tables 2

and 3 were used for the lattice parameter calculation. One possible explanation for the above change is that there are no oxygen vacancies above GOM due to Eq. (2) on the basis that it is valid near GOM. In this case, the crystal is regarded as hyperstoichiometric in this region.

## References

[1] T.B. Lindemer, A.L. Sutton Jr., J. Am. Ceram. Soc. 71 (1988) 553.
[2] K. Une, M. Oguma, J. Nucl. Mater. 115 (1983) 84.
[3] A.E. Martin, R.K. Edwards, J. Phys. Chem. 69 (1965) 1788.
[4] E.K. Storms, J. Nucl. Mater. 132 (1985) 231.
[5] K. Une, M. Oguma, J. Nucl. Mater. 131 (1985) 88.
[6] K. Une, S. Kashibe, J. Nucl. Mater. 189 (1992) 210.
[7] M. Hirai, J.H. Davies, R. Williamson, J. Nucl. Mater. 226 (1995) 238.
[8] J.S. Anderson, K.D.B. Johnson, J. Chem. Soc. (1953) 1731.
[9] T. Fujino, J. Tateno, H. Tagawa, J. Solid State Chem. 24 (1978) 11.
[10] P.T. Sawbridge, C. Baker, R.M. Cornell, K.W. Jones, D. Reed, J.B. Ainscough, J. Nucl. Mater. 95 (1980) 119.
[11] S. Kemmler-Sack, W. Rüdorff, Z. Anorg. Allg. Chem. 354 (1967) 255.
[12] T. Fujino, K. Naito, J. Inorg. Nucl. Chem. 32 (1970) 627.
[13] T. Fujino, N. Sato, K. Fukuda, in: Proceedings of the 1997 International Topical Meeting on LWR Fuel Performance, Portland, March 2–6 1997, p. 565.
[14] T. Fujino, N. Sato, K. Yamada, T. Shiratori, K. Fukuda, H. Serizawa, in: Proceedings of the 2000 International Topical Meeting on LWR Fuel Performance, Park City, April 9-13, 2000, p. 641.
[15] H.R. Hoekstra, S. Siegel, E.X. Gallagher, J. Inorg. Nucl. Chem. 32 (1970) 3237.
[16] DATABASE MALT2, The Japanese Society of Calorimetry and Thermal Analysis, 1987.
[17] D.E. Williams, Ames Lab. Rep. IS-1052 (1964).
[18] S.R. Dharwadkar, M.S. Chandrasekharaiah, Anal. Chim. Acta 45 (1969) 545.
[19] T. Fujino, T. Yamashita, Fresenius Z. Anal. Chem. 314 (1983) 156.
[20] T. Fujino, C. Miyake, in: A.J. Freeman, C. Keller (Eds.), Handbook on the Physics and Chemistry of the Actinides, vol.6, p.155, North-Holland, Amsterdam, 1991.
[21] J. Tateno, T. Fujino, H. Tagawa, J. Solid State Chem. 30 (1979) 265.
[22] T. Fujino, N. Sato, K. Yamada, S. Nakama, K. Fukuda, H. Serizawa, T. Shiratori, J. Nucl. Mater. 265 (1999) 154.
[23] T. Fujino, N. Sato, K. Yamada, J. Nucl. Mater. 247 (1997) 265.
[24] T. Fujino, S. Nakama, N. Sato, K. Yamada, K. Fukuda, H. Serizawa, T. Shiratori, J. Nucl. Mater. 246 (1997) 150.
[25] I. Cohen, R.M. Berman, J. Nucl. Mater. 18 (1966) 77.
[26] Y. Hinatsu, T. Fujino, J. Solid State Chem. 68 (1987) 255.
[27] T. Yamashita, T. Fujino, H. Tagawa, J. Nucl. Mater. 132 (1985) 192.
[28] Y. Hinatsu, T. Fujino, J. Solid State Chem. 73 (1988) 388.
[29] T. Yamashita, T. Fujino, J. Nucl. Mater. 136 (1985) 117.
[30] T. Fujino, T. Yamashita, H. Tagawa, J. Solid State Chem. 73 (1988) 544.
[31] S. Fukushima, T. Ohmichi, A. Maeda, H. Watanabe, J. Nucl. Mater. 105 (1982) 201.
[32] T. Ohmichi, S. Fukushima, A. Maeda, H. Watanabe, J. Nucl. Mater. 102 (1981) 40.
[33] W. Rüdorff, H. Erfurth, S. Kemmler-Sack, Z. Anorg. Allg. Chem. 354 (1967) 273.
[34] T. Fujino, N. Sato, J. Nucl. Mater. 282 (2000) 232.